Title

TEMPERATURE DEPENDENT HARTREE-POCK-BOGOLIUBOV CALCULATIONS IN HOT ROTATING NUCLEI

Authors

Egido, J.L.
Ring, P.
Mang, H.J.

Publication Date

1985-06-01

LBL-19785
Preprint

Lawrence Berkeley Laboratory
UNIVERSITY OF CALIFORNIA

Submitted to Nuclear Physics A

TEMPERATURE DEPENDENT HARTREE-FOCK-BOGOLIUBOV CALCULATIONS IN HOT ROTATING NUCLEI

J.L. Egido, P. Ring and H.J. Mang

June 1985

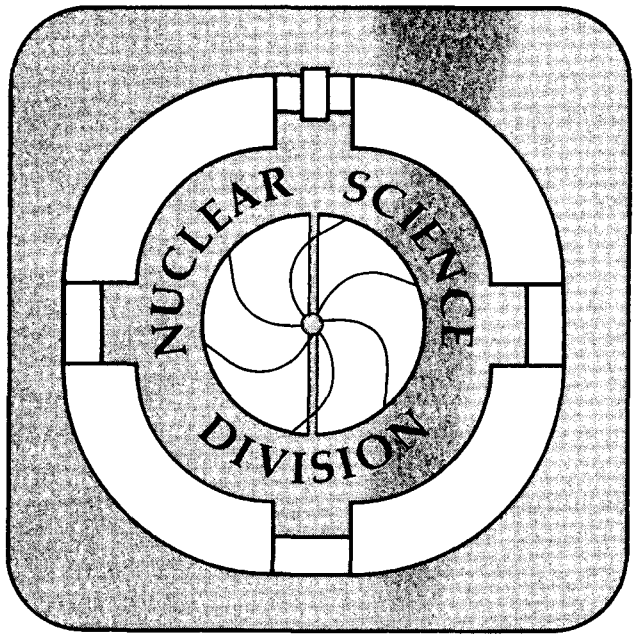

Prepared for the U.S. Department of Energy under Contract DE-AC03-76SF00098

DISCLAIMER

LBL-19785

Temperature Dependent Hartree-Fock-Bogoliubov Calculations in Hot Rotating Nuclei*

J.L. Egido,† P. Ring‡

Nuclear Science Division
Lawrence Berkeley Laboratory
University of California
Berkeley, California 94720

and

H.J. Mang

Physikdepartment der Technischen
Universität München
D-8046
Garching, West Germany

†Permanent address: Departmento de Fisica Teorica, Universidad Autonoma de Madrid, Spain

‡Permanent address: Physikdepartment der Technischen Universität München, West Germany

*This work was supported in part by the CAICYT, Spain, a Fulbright/MEC grant, the Bundesministerium für Forschung und Technologie, the Deutsche Forschungsgemeinschaft and by the Director, Office of Energy Research, Division of Nuclear Physics of the Office of High Energy and Nuclear Physics of the U.S. Department of Energy under Contract DE-AC03-76SF00098.

LBL-19785

Temperature Dependent Hartree-Fock-Bogoliubov Calculations in Hot Rotating Nuclei*

J.L. Egido,† P. Ring‡

Nuclear Science Division
Lawrence Berkeley Laboratory
University of California
Berkeley, California 94720

and

H.J. Mang

Physikdepartment der Technischen
Universität München
D-8046
Garching, West Germany

Abstract:

Cranked temperature dependent Hartree-Fock Bogoliubov (CTHFB) equations in the rotating frame are solved numerically for a realistic case in the Rare Earth region, the nucleus ^{164}Er. The behavior of pairing correlations, shape degrees of freedom and other physical quantities are discussed as a function of angular momentum and temperature.

†Permanent address: Departmento de Fisica Teorica, Universidad Autonoma de Madrid, Spain

‡Permanent address: Physikdepartment der Technischen Universität München, West Germany

*This work was supported in part by the CAICYT, Spain, a Fulbright/MEC grant, the Bundesministerium für Forschung und Technologie, the Deutsche Forschungsgemeinschaft and by the Director, Office of Energy Research, Division of Nuclear Physics of the Office of High Energy and Nuclear Physics of the U.S. Department of Energy under Contract DE-AC03-76SF00098.

1. INTRODUCTION

Within the last few years an increasing number of experimental studies has been devoted to the investigation of highly excited compound states in nuclei formed after a HI-fusion reaction (for a recent review see ref. 1). Two parameters characterize this region, the excitation energy and the angular momentum. A number of new features are expected, such as phase transitions and changes of the nuclear shape.

For very high excitation energies the nucleus should behave like a hot classical droplet: At not too high angular velocities it should have a slightly oblate shape and should rotate around its symmetry axis. Pairing correlations should have disappeared and a rigid moment of inertia is expected.

At small excitation energies, near to the yrast line one has a quantum mechanical behavior: discrete levels forming rotational bands of different character, which can be studied by the gamma-radiation following a HI-xn reaction. Nuclei, which are well deformed and superfluid in the ground state, rotate perpendicular to the symmetry axis and the moment of inertia is largely reduced by the pairing correlations at least for small angular velocities. Level crossings are observed and alignment phenomena play a crucial role.

The investigations in this paper are devoted to the transition region between the discrete levels at the yrast line and the classical regime, where pairing correlations have vanished. This region is characterized by a steeply rising level density as a function of the excitation energy. It is therefore meaningless to describe this regime in terms of discrete bands. Since the lifetime of such a compound state is sufficiently large we can assume that in this region of high level densities one has a thermodynamical equilibrium, which allows us to describe the nucleus in this region by a statistical

ensemble with a fixed temperature. It is clear that this method breaks down in the vicinity of the yrast line, in particular, trivially below the energy gap of 2Δ, but already at a few MeV excitation energy above yrast this concept is well justified.

As an additional approximation we use mean-field theory with constraints on the physically important quantum numbers as particle number and angular momentum, i.e. we use the Cranking model. This approximation has been used in nearly all microscopic investigations at the yrast line (for a review see ref. 2) and has proven to be very useful. In a sense it is a classical approximation, which works for two reasons: the residual interaction is strong and there is a large number of particles participating in the collective process of rotation. At finite temperatures this approximation should be even better, because the high level density gives an additional justification for a classical behaviour.

Following all these arguments we use in this paper Cranked Temperature dependent Hartree-Fock-Bogoliubov (CTHFB) theory and we apply it to a realistic case, the nucleus ^{164}Er, a typical example for a well deformed axially symmetric heavy nucleus, which shows relatively strong pairing at the ground state, and which has been much under investigation both experimentally and theoretically. In fact Cranking theory has proven to be a very powerful tool to describe its properties along the yrast line and low lying rotational bands in its vicinity[3,4,5]).

Temperature dependent BCS and HFB theory was introduced many years ago[6-9]). The later has the two well known limits of temperature dependent BCS-theory, where a fixed deformation is assumed and temperature dependent HF-theory[10]), where the pairing correlations are neglected. Both have been

used considerably in the seventies[11-13]). For the description of a rotating nucleus Cranked temperature dependent HFB theory is needed. It has been discussed in the framework of perturbation theory[14]) and in exactly soluble models[15,16]).

The first application to a realistic case in the framework of the cranking model has been carried out by Tanabe et al[17,18]). It turned out that in cases of negative quasi-particle energies, which occur in the region of band-crossings[19]), CTHFB-theory does not give the proper limit for T = 0, where one should find the usual Cranked HFB-results. Tanabe et al therefore extended CTHFB-theory by projecting onto good parity and onto good number parity. They thus obtain the proper limit for small temperatures. On the other side, because of the increased numerical difficulties connected with this projection, additional approximations have been introduced for the solution of the variational equations. Therefore the full CTHFB equations have not been solved so far for realistic heavy nuclei. In this paper we present such a solution. We do not project onto good parity nor onto good number parity, i.e. we do not find the proper limit at small temperatures. We think, however, that this is not a crucial point, because at very small excitation energies, where projection causes differences, a description in the framework of a temperature is not meaningful anyhow, because in this region the level density is too low. This simple fact can not be improved by projection. On the other side neglecting the projection allows us an easier solution of the exact CTHFB equations. We find several differences to ref. 18 even at the highest temperatures.

THFB-theory has been described in great detail by many authors[16,17,18]). We therefore give in Section 2 only the final equations used in our

calculations. We also discuss in this section the technique by which we solve the equations. In Section 3 we present details of our model and discuss the results for the nucleus ^{164}Er. Section 4 contains a summary and concluding remarks.

2. THE TEMPERATURE DEPENDENT HARTREE-FOCK-BOGOLIUBOV EQUATIONS

The CTHFB-equations have formally the same structure as ordinary Cranked-HFB-equations. We can write them down in the form of a nonlinear eigenvalue problem given by Baranger[20]:

$$\begin{pmatrix} h & \Delta \\ -\Delta^* & -h^* \end{pmatrix} \begin{pmatrix} U \\ V \end{pmatrix}_k = E_k \begin{pmatrix} U \\ V \end{pmatrix}_k \tag{1}$$

The CTHFB-matrix contains the potential h in the ph-channel

$$h = \varepsilon - \lambda_p N_p - \lambda_n N_n - \omega J_x + \Gamma \tag{2}$$

with the single particle energies ε, the Coriolis field ωJ_x, the number operators for protons and neutrons N_p and N_n and the selfconsistent field

$$\Gamma_{kk'} = \sum_{\ell\ell'} v_{k\ell'k'\ell} \rho_{\ell\ell'} \tag{3}$$

The pairing potential in the pp-channel is defined as usual

$$\Delta_{kk'} = \frac{1}{2} \sum_{\ell\ell'} v_{k\ell'\ell'\ell} \kappa_{\ell\ell'} \tag{4}$$

The difference to simple HFB-equations consists in the densities which are now thermal averages over a statistical ensemble of multi-quasiparticle states:

$$\rho_{kk'} = (U\, f\, U^\dagger + V^*(1 - f)V^T)_{kk'} \tag{5}$$

and

$$\kappa_{kk'} = (U\ f\ V^{\dagger} + V^{*}(1 - f)U^{T})_{kk'} \tag{6}$$

They contain the temperature dependent occupation factors for quasiparticles:

$$f_k = 1/(1 + \exp(E_k/T)) \tag{7}$$

which are zero for normal HFB-theory.

The diagonalization of the HFB-matrix gives us quasiparticle energies E_k and a quasiparticle basis, i.e. the HFB-coefficients U_{mk} and V_{mk}, which define the quasiparticle operators via the general Bogoliubov transformation

$$\alpha_k^{\dagger} = \sum_m U_{mk} c_m^{\dagger} + V_{mk} c_m \tag{8}$$

Having this basis we can calculate the densities ρ and κ in the eqs.(5) and (6) and the potentials Γ and Δ.

To obtain a closed system we finally have to specify the constraints, which determine the Lagrange parameters λ_p, λ_n and ω

$$\langle N_n \rangle = N \qquad \langle N_p \rangle = Z \tag{9}$$

$$\langle J_x \rangle + \omega \mathcal{J}_c = \sqrt{I(I+1)} \tag{10}$$

where $\mathcal{J}_c$ is eventually a core moment-of-inertia.

The temperature dependent HFB-equations can be derived in different ways, by Greens-function techniques[6]), by a variation of the grand canonical potential[21,8,17]) or as a stationary solution of the temperature- and

time-dependent Hartree-Fock-Bogoliubov equations[22]), which are obtained from the equation of motion for the generalized densities ρ and κ in eq.(10) in connection with a Wick theorem for thermal averages[23,24]).

The numerical solution of the CTHFB-equations can be carried out in a similar way as the solution of the normal HFB-equations, where several techniques have been used.

The most obvious way is an iterative diagonalization[25]): one starts with an initial guess for the potentials Γ and Δ as for instance a deformed Nilsson potential with a reasonable deformation and reasonable gap parameters and diagonalizes the linear eigenvalue problem (1) adjusting the chemical potential and the cranking frequency ω in such a way that the constraints (9) and (10) are fulfilled. One thus finds quasiparticle energies and HFB-wavefunctions for the first step of an iteration. They are used to calculate the occupation probabilities (7) and the densities (5) and (6). In the next step one uses these densities to calculate new potentials Γ and Δ in eqs.(3) and (4), and so forth until convergence is achieved. The criterium for convergence was that the total energy and all eigenvalues of eq.(1) differ by less than 10 eV in two subsequent steps of the iteration. It is well known that this method is not very effective in the regions of level crossings[19]), because in a normal HFB-problem one has to choose in each step of the iteration the appropriate occupation, which might be a tricky problem in the level crossing region. It therefore has been replaced in many applications of the Cranked HFB-theory by the steepest descent method[26,3]), where a change of the occupation can not be achieved in one step of the iteration (it actually would require a step with an infinite size).

The method of steepest descent has been extended in ref. 18 to finite temperatures. This involves considerable complications, because now one has to calculate in addition to the gradient with respect to two-quasiparticle excitations ($\alpha^\dagger\alpha^\dagger$) also the gradient with respect to rearrangements of the quasiparticles in the statistical average ($\alpha^\dagger\alpha$) and the gradient with respect to the occupation factors f_k. In ref. 18 only the gradient with respect to the two-quasiparticle excitations was taken into account fully; the other two gradients were treated in an approximative way. Therefore only an approximate solution of the full CTHFB-equations was obtained.

In this paper we used for the solution of the full CTHFB equations the method of iterative diagonalization, which is much simpler than the gradient-method in this case. Since the occupation is always determined by the temperature we do not have convergence problems. At finite temperatures the level-crossings are washed out. We are certainly not able to describe backbending at the yrast-line properly, but as discussed in the introduction the use of a temperature is anyhow not meaningful close to the yrast-line.

3. NUMERICAL RESULTS

For a realistic application of Cranked THFB-theory we use the configuration space and the effective interaction of Kumar and Baranger[27]). An inert core of 40 protons and 70 neutrons is surrounded by the valence protons in the spherical oscillator shells N = 4 and 5 and by the valence neutrons in the shells N = 5 and 6. The valence particles interact via separable forces, namely a quadrupole-quadrupole force in the ph-channel and monopole pairing forces in the pp-channel:

$$H = \varepsilon - \frac{\chi}{2} Q^{\dagger}Q - G_p P_p^{\dagger} P_p - G_n P_n^{\dagger} P_n \tag{11}$$

ε are spherical single-particle energies, Q is the quadrupole operator and $P_{p,n}^{\dagger}$ create Cooper pairs for protons and neutrons. The force-parameter G_p, G_n and χ are adjusted to the groundstate properties of the Rare Earth nuclei. Details are given in ref. 27.

In Fig. 1 we show the internal energy $E = \langle H \rangle + \frac{\omega^2}{2} \mathcal{J}_c$ for constant temperatures (isothermal lines) and for constant entropy (isentropic lines):

$$S = -\sum_k (f_k \ln f_k + (1 - f_n) \ln(1 - f_k)) \tag{14}$$

The isothermal lines are more or less parallel to the yrast line. They increase for all temperatures monotonically with the angular momentum. We do not find minima at finite low spins even for higher temperatures as they have been found in ref. 18, i.e. we do not find the new phase transition discussed in refs. 28,29. We do not think that this different behavior, which shows up only at higher temperatures, is caused by the slight differences in configuration space and in the residual interaction nor by the projection onto

good parity and number parity in ref. 18, but we believe that the minima in Fig. 1 of ref. 28, which the authors understand as an indicator of a new phase transition called "bidirectional alignment," are caused by the approximation used in the numerical solution of the CTHFB-equations.

The isentropic lines behave in great extent as the isothermal. Only for small angular momentum and small excitation energies are the slopes different. For all other values of E and I they are parallel. That means that the question isentropic or isothermal rotation is mostly of academic interest.

In Fig. 2 we present the internal energy as a function of the temperature for different values of the angular momentum. For high angular momenta ($I > 30\hbar$) these curves are nearly parallel. At low spins we observe a sudden increase of the internal energy in the region of $T = 0.5$ (MeV). It has its origin in the pairing collapse in this temperature region, which we will discuss in the following.

In Figs. 3 and 4 we show the pairing gap parameters for protons and neutrons as a function of the angular momentum for different temperatures. We observe a pairing collapse as a function of the angular momentum as well as a pairing collapse as a function of the temperature. The critical angular momenta for zero temperature are $I = 30\hbar$ for the neutrons and $I = 50\hbar$ for the protons. The critical temperatures at zero spin are $T = 0.5$ (MeV) in both cases. This twofold phase-transition with increasing temperature and increasing angular momentum (i.e. increasing angular velocity) is in complete analogy to the transition from the superconducting phase to the normal conducting phase in a solid with increasing temperature and with increasing external magnetic field, which violates time reversal symmetry and breaks

Cooper-pairs in the same way as the Coriolis field in a rotating nucleus. With increasing temperature more and more blocked many-quasiparticle configurations are populated, which diminishes pairing. These two phase transitions have been discussed earlier in model calculations[16]) and in realistic nuclei[18,22]) and the results obtained in this paper are more or less in agreement with these earlier investigations.

In mean field theory, which is used in our calculations, these phase transitions are very sharp as one expects in an infinite system. We have to keep in mind, however, that real nuclei are finite systems and in reality these transitions might be smeared out considerably by fluctuations. At zero temperature one has only quantum fluctuations: In this case there exist calculations which go beyond the mean-field approach and which take into account explicitly fluctuations connected with the violation of number symmetry by number projection[30-32]) and fluctuations connected with the virtual admixture of pairing vibrations by the Generator Coordinate Method[33]). Theey indicate that the sharp phase transition found in mean-field theory is considerably washed out in finite nuclei. For increasing temperatures one has in addition thermal fluctuations, which cause an additional smearing[11,34,35]).

In Fig. 5 we show the deformation parameter β for the selfconsistent solution of the CTHFB equations as a function of the temperature. We study the region of $T \leq 1$ (MeV). In this temperature region the nucleus ^{164}Er turns out to be very stiff against shape changes. With increasing temperature we find only very small changes in β, there is only a small tendency to spherical shapes at the highest temperatures under consideration as one would expect in a classical picture. In the region of small spins ($I < 30\hbar$) we

find at temperatures T < 0.5 (MeV) first an increasing deformation. This is clearly connected with the Coriolis-anti-Pairing effect in this region: Increasing temperature decreases pairing, which in turn allows the nucleus to become more deformed. Such an effect is no longer seen for angular momenta beyond the pairing collapse.

At very small temperatures (T < 0.1 MeV) we observe for the higher spins a small kink. It has its origin in the fact that the smallest finite temperature for which we solved the CTHFB-equations was T = 0.05 (MeV). As discussed in the introduction there is no continuous connection to the calculation with T = 0. This shortcoming could in principle be eliminated by projection onto parity and number parity[17]), which we did not carry out, because in this energy region the description by a temperature dependent theory is not justified at all.

The nucleus ^{164}Er is for all temperatures under consideration also relatively stiff against γ-deformations as we see in Fig. 6. For small temperatures we find increasing γ-values for increasing spin. This behavior has been observed in many calculations in this region[25,19,31]). It contradicts the classical picture, where one expects the nucleus to flatten more in the direction of the rotational axis, which would correspond to negative γ-values. This unexpected behavior is obviously connected with the shell structure, and we find that it disappears more and more with increasing temperature.

In Fig. 7 we show the moment-of-inertia defined as

$$\mathcal{J} = \frac{\langle J_x \rangle}{\omega} \qquad (13)$$

For small temperatures and small spin values we have pairing correlations, which produce the well known reduction of Δ in this region. For $T > 0.5$ (MeV) pairing has collapsed and we find rather constant moments of inertias for all spin values, somewhat larger than the rigid body value. For small temperatures we find a steep increase of the moment-of-inertia between 10 and 20$\hbar$. It is well known that it is connected with the sudden alignment of a $i_{13/2}$ pair of neutrons, which produces backbending at the yrast line. As discussed in section 2 our method to solve the CTHFB-equations cannot reproduce this in all details, but we reproduce the main feature, namely the sharply rising moment-of-inertia. Around angular momentum 30$\hbar$ we observe a second increase, obviously connected with proton alignment in the $h_{11/2}$ orbit.

In Fig. 8 we plot the moment of inertia as a function of the temperature T for constant angular momenta. Again we observe the reduction due to pairing at small angular momenta and temperatures, which disappears with increasing temperature and angular momentum.

The entropy S of eq.(14) is plotted in Fig. 9 as a function of the temperature. For large temperatures we find for all angular momenta the same entropy. For angular momenta smaller than 30$\hbar$ we find a substantial lowering with decreasing temperature, connected with the pairing correlation in this region. Higher pairing means increased order and smaller entropy. We also find a kink at $T = 0.05$ (MeV) for large angular momenta. It has the same origin as the kink in Fig. 5 and shows that the description by a temperature breaks down in this region. Obviously we should have a smooth connection with the origin in Fig. 9. From Fig. 1 we see that $T = 0.05$ corresponds indeed to a very small excitation energy above the yrast line, i.e. to a region where the level density is too low as to justify a temperature dependent description.

4. SUMMARY AND CONCLUSIONS

For the first time the full Cranked temperature dependent HFB-equations are solved numerically exactly in a realistic case. Projection onto parity and number parity proposed in ref. 17 has been neglected, because it is only important for very low temperatures and high spins, i.e. in a region where probably a description of the nucleus by a thermal equilibrium is not justified anyhow.

The full solution of the CTHFB-equations is carried out numerically by iterative diagonalization, which is considerably simpler than a gradient method for the case of finite temperatures. Problems with level crossings, which inhibit this method for the accurate description of the yrast line, do not exist at finite temperatures, because the occupation of the quasiparticle levels is smeared out in this region. A small and completely negligible drawback of the method is that we do not have a continuous connection to the $T = 0$ limit.

The results obtained in this calculation are in qualitative agreement with earlier model calculations and in many points also in agreement with earlier non fully selfconsistent investigations[22]) and with work by Tanabe et al[18]) where the CTHFB-equations have been solved approximately. There are, however, some essential differences. In particular we do not find any indication of the new phase transition called "bidirectional alignment" proposed in refs. 28 and 29.

ACKNOWLEDGEMENTS

Two of the authors (J.L.E. and P.R.) would like to express their gratitude to J.O. Rasmussen and the Nuclear Science Division for the generous hospitality extended to them during their stay at the Lawrence Berkeley Laboratory.

This work was supported in part by the CAICYT, Spain, a Fulbright/MEC grant, the Bundesministerium für Forschung und Technologie, the Deutsche Forschungsgemeinschaft and by the Director, Office of Energy Research, Division of Nuclear Physics of the Office of High Energy and Nuclear Physics of the U.S. Department of Energy under Contract DE-AC03-76SF00098.

FIGURE CAPTIONS

Fig. 1 The energy of the nucleus ^{164}Er as a function of the angular momentum. Full lines are isothermal lines and correspond to constant temperatures (the units are MeV) with T = 0.0, 0.1, 0.2, ..., 1.0, dashed lines are isentropic lines and correspond to constant entropy with S = 0, 5, 10, ..., 30.

Fig. 2 The energy of the nucleus ^{164}Er as a function of the temperature for different angular momenta.

Fig. 3 The gap parameter for the neutrons in the nucleus ^{164}Er as a function of the angular momentum for different temperatures (in units of MeV). For all temperatures $T \geq 0.5$ MeV the gap vanishes.

Fig. 4 The gap parameter for the protons in the nucleus ^{164}Er as a function of the angular momentum for different temperatures (in units of MeV). For all temperatures $T \geq 0.6$ MeV the gap vanishes.

Fig. 5 The deformation parameter β in the nucleus ^{164}Er as a function of the temperature for different angular momenta.

Fig. 6 The deformation parameter γ (in degrees) in the nucleus ^{164}Er as a function of the angular momentum for different temperatures (in units of MeV).

Fig. 7 The moment of inertia of the nucleus ^{164}Er as a function of the angular momentum for different temperatures (in units of MeV).

Fig. 8 The moment of inertia of the nucleus ^{164}Er as a function of the temperature for different angular momenta.

Fig. 9 The entropy of the nucleus ^{164}Er as a function of the temperature for different values of the angular momenta (I = 0, 6, 12, ..., 54$\hbar$).

REFERENCES

1. B. Herskind; Nucl. Structure and Heavy Ion Dynamics, LXXXVII Corso, Soc. Italiana de Fisica, Bologna, Italy, 1984, p. 68
2. A. Goodman; Adv. Nucl. Phys., ed. J. Negele and E. Voigt, Vol. 11 (Plenum Press, New York, 1979)
3. J.L. Egido, H.J. Mang, and P. Ring; Nucl. Phys. A339 (1980) 390
4. J.L. Egido, H.J. Mang, and P. Ring; Nucl. Phys. A341 (1980) 229
5. Y.R. Shimizu and K. Matsuanagi; Prog. Theor. Phys. 70 (1983) 144
6. M. Sano and S. Yamasaki; Prog. Theor. Phys. 29 (1963) 397
7. T. Kammuri; Prog. Theor. Phys. 31 (1964) 595
8. A.L. Goodman; Nucl. Phys. A352 (1981) 30
9. A.L. Goodman; Nucl. Phys. A352 (1981) 45
10. J. des Cloizeaux, in Many-Body Physics, ed. C. de Witt and R. Balian, (Gordon & Breach, New York, 1968)
11. L.G. Moretto; Phys. Lett. 46B (1973) 20
12 M. Brack and Ph. Quentin; Physica Scripta 10A (1974) 163
13. U. Mosel, P.G. Zint, and K.H. Passler; Nucl. Phys. A236 (1974) 252
14. M. Sano and M. Wakai; Prog. Theor. Phys, 48 (1972) 160
15. A.L. Goodman; Nucl. Phys. A369 (1981) 365
16. A.L. Goodman; Nucl. Phys. A370 (1981) 90
17. K. Tanabe, K. Sugaware-Tanabe, and H.J. Mang; Nucl. Phys. A357 (1981) 20
18. K. Tanabe, K. Sugaware-Tanabe, and H.J. Mang; Nucl. Phys. A357 (1981) 45
19. B. Banerjee, H.J. Mang, and P. Ring; Nucl. Phys. A215 (1973) 366
20. M. Baranger; Phys. Rev. 120 (1980) 957
21. H.C. Lee and S. Das Gupta; Phys. Rev. C19 (1979) 2369
22. P.Ring, L.M. Robledo, J.L. Egido, and M. Faber; Nucl. Phys. A419 (1984) 261

23. M. Gaudin; Nucl. Phys. 15 (1960) 89

24. A. Fetter and J.D. Walecka, Quantum Theory of Many-Particle Systems (McGraw-Hill, San Francisco, 1971)

25. P. Ring, R. Beck, and H.J. Mang; Z. Phys. 231 (1970) 10

26. H.J. Mang, B. Samadi, and P. Ring; Z. Phys. A279 (1976) 325

27. B. Baranger and K. Kumar; Nucl. Phys. A110 (1968) 490

28. K. Tanabe and K. Sugawara-Tanabe; Phys. Lett. 97B (1980) 337

29. K. Tanabe and K. Sugawara-Tanabe; Nucl. Phys. A390 (1981) 385

30. A. Faessler, K.R. Sandya Devi, F. Gruemmer, K.W. Schmid, and R.R. Hilton; Nucl. Phys. A256 (1976) 106

31. J.L. Egido and P. Ring; Nucl. Phys. A388 (1982) 19

32. U. Mutz and P. Ring; J. Phys. G10 (1984) L39

33. F.L. Canto, P. Ring, and J.O. Rasmussen; Phys. Lett. to be published

34. A.L. Goodman; Phys. Rev. C29 (1984) 1887

35. J.L. Egido, P. Ring, S. Iwasaki, and H.J. Mang; Phys. Lett. 154B (1985) 1

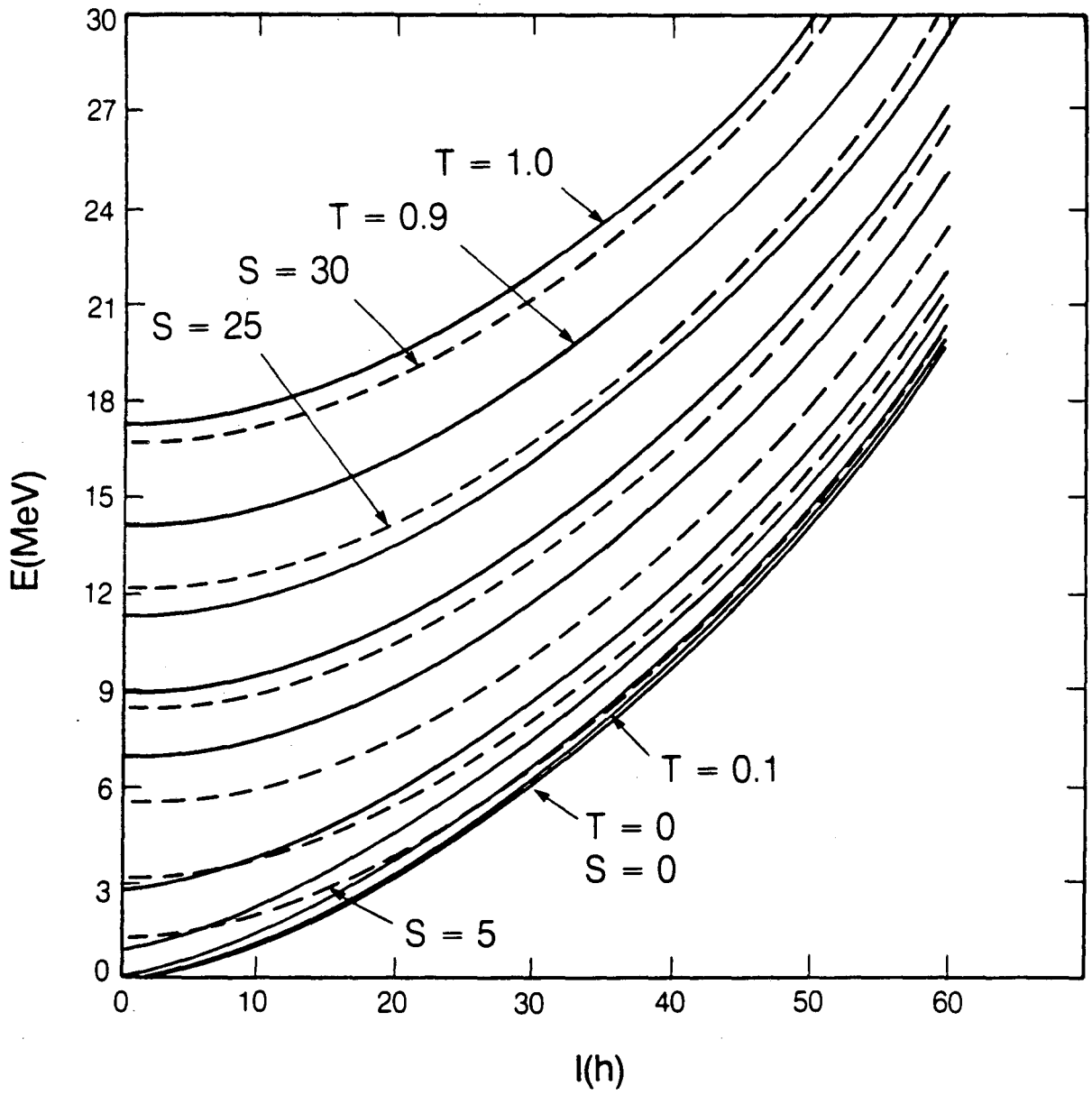

Fig. 1

XBL 856-9559

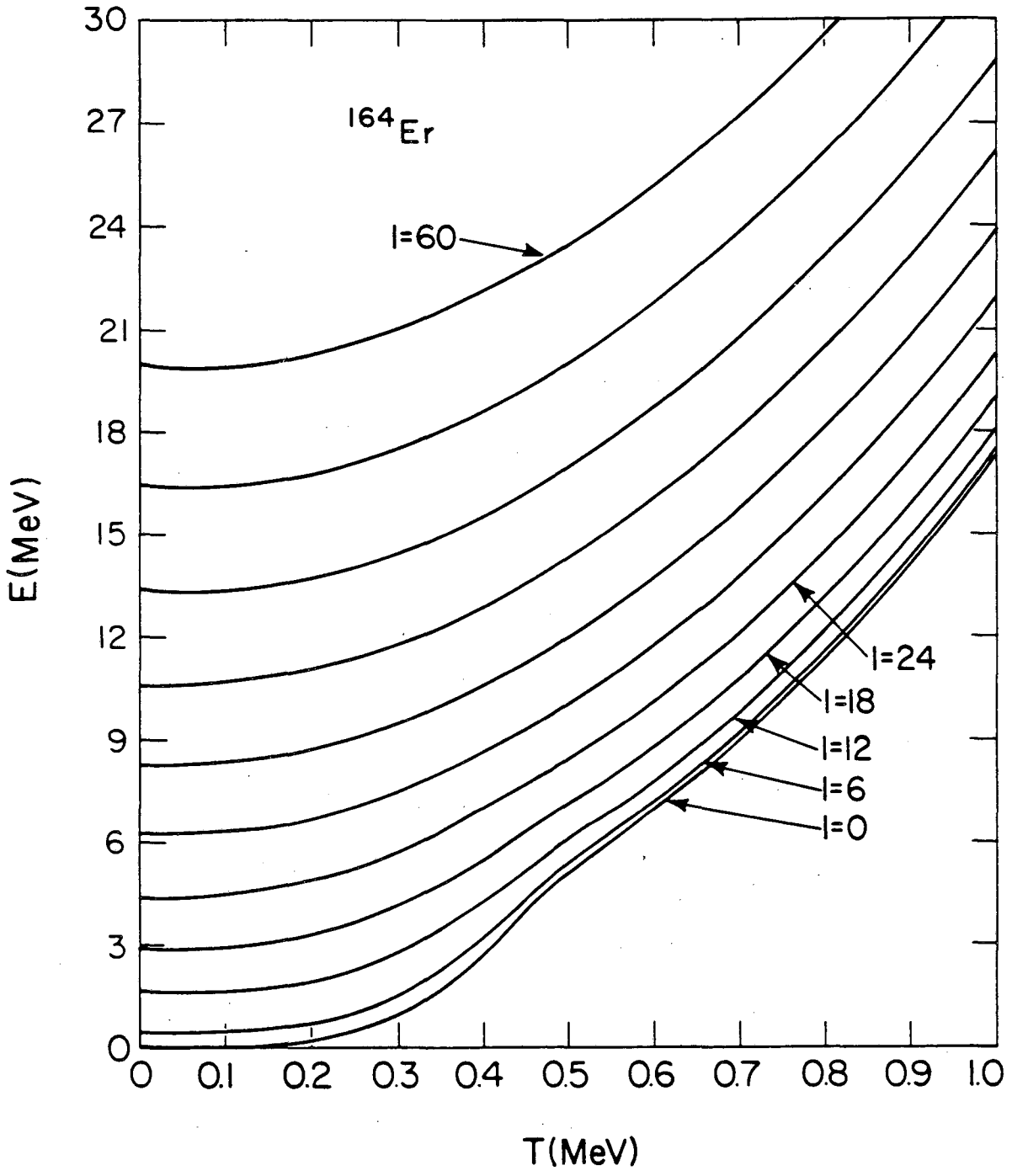

Fig. 2

XBL 8411-6383

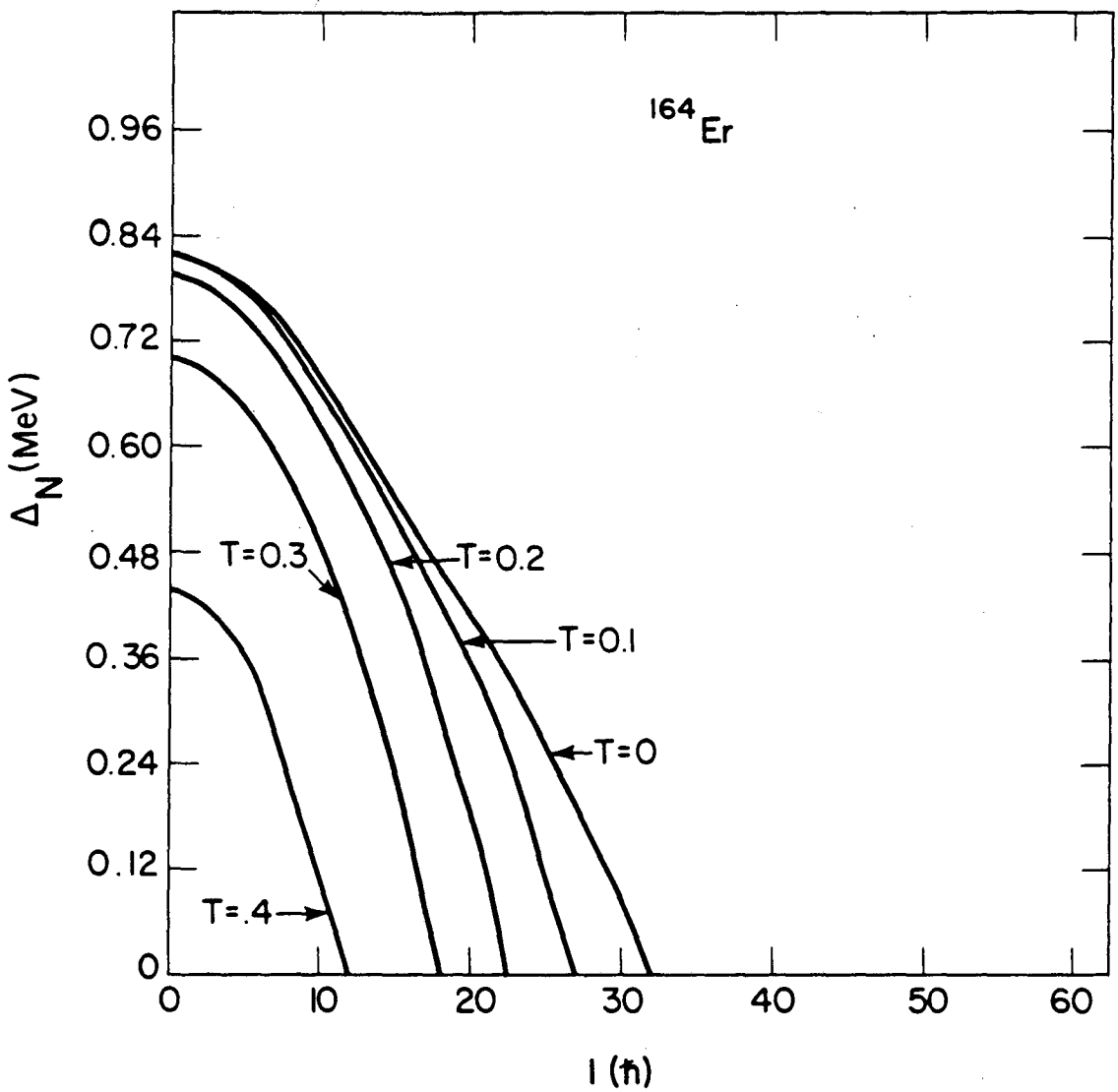

Fig. 3

XBL 8411-6386

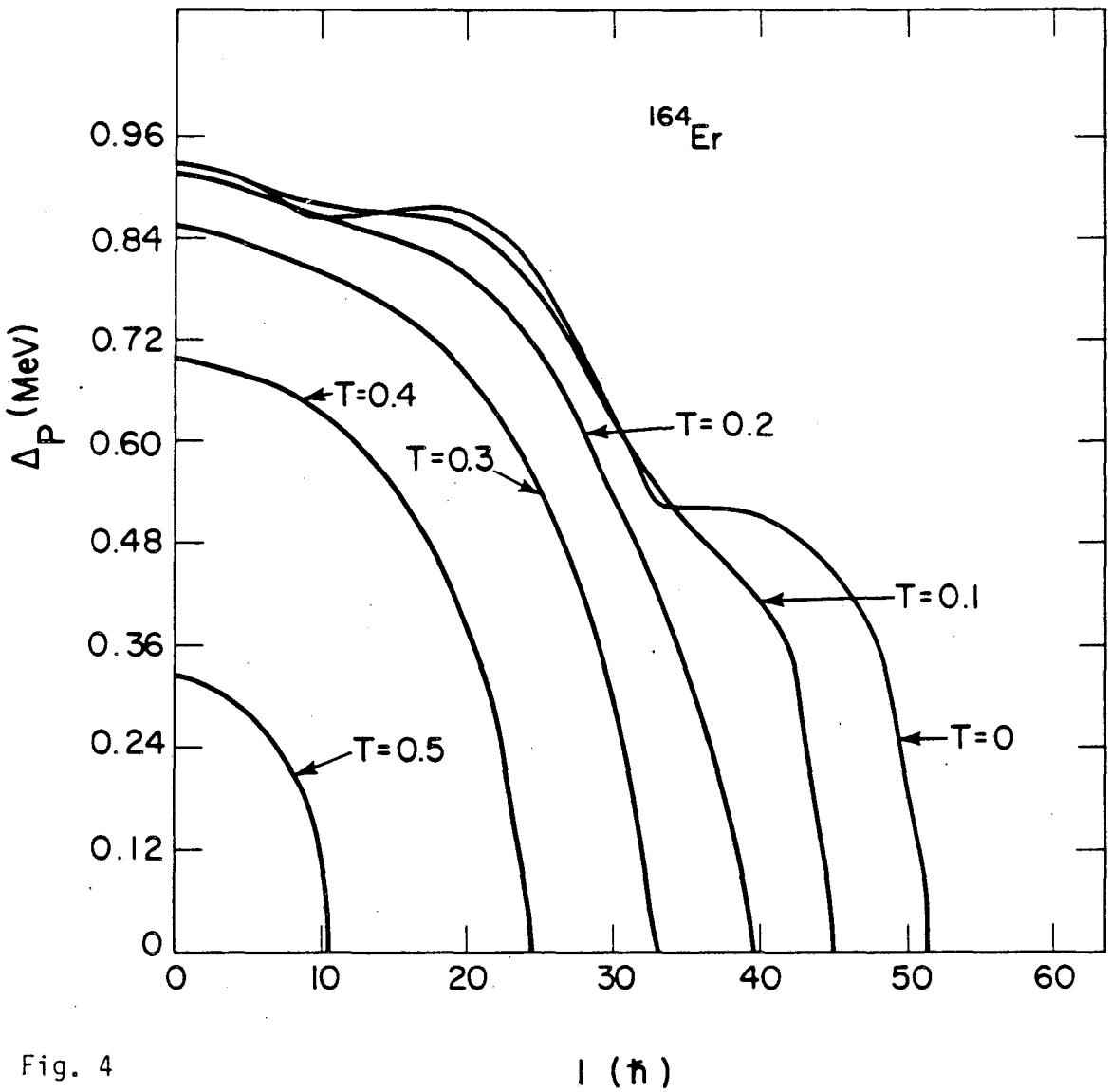

Fig. 4

XBL 8411-6385

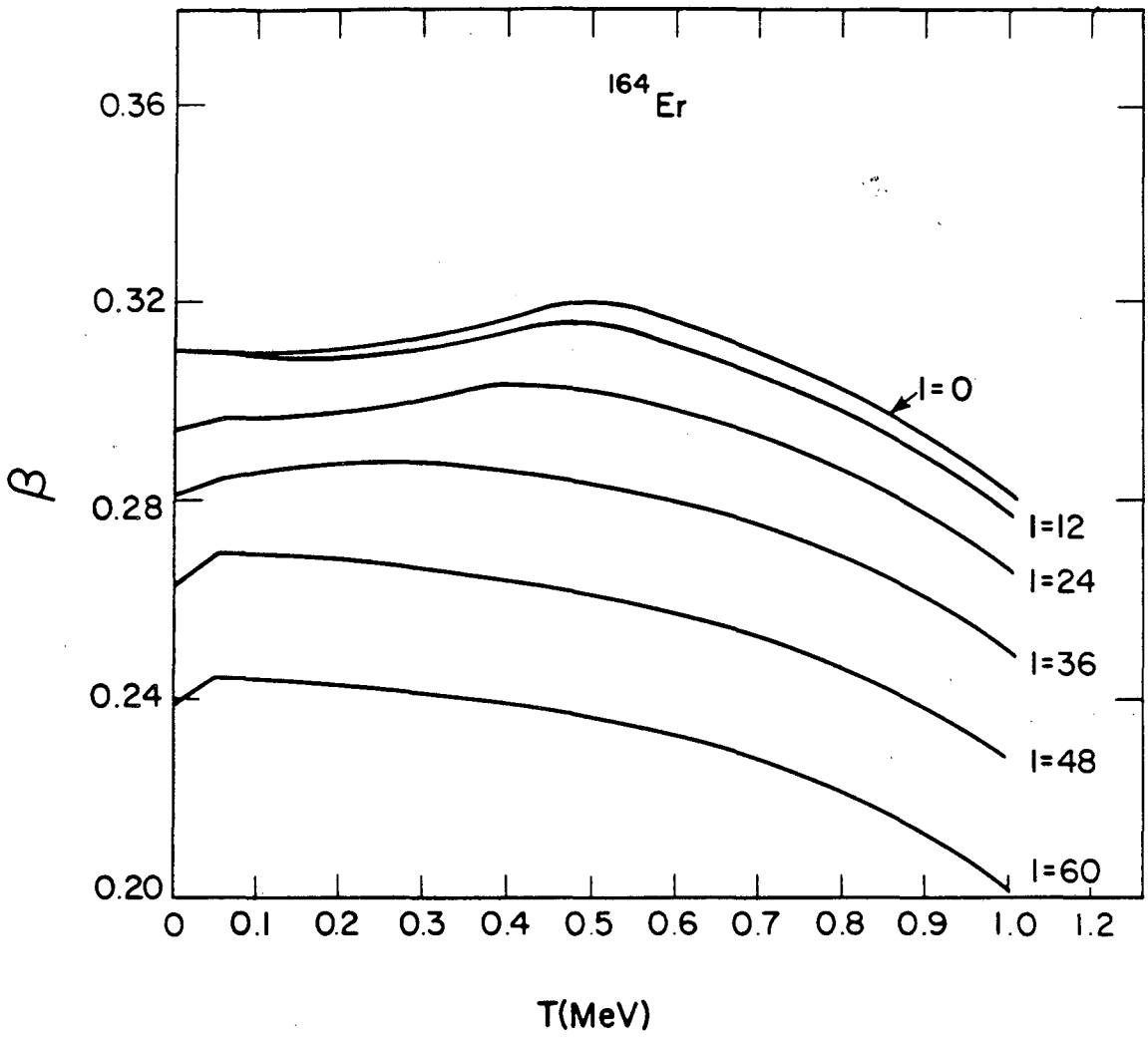

Fig. 5

XBL 8411-6397

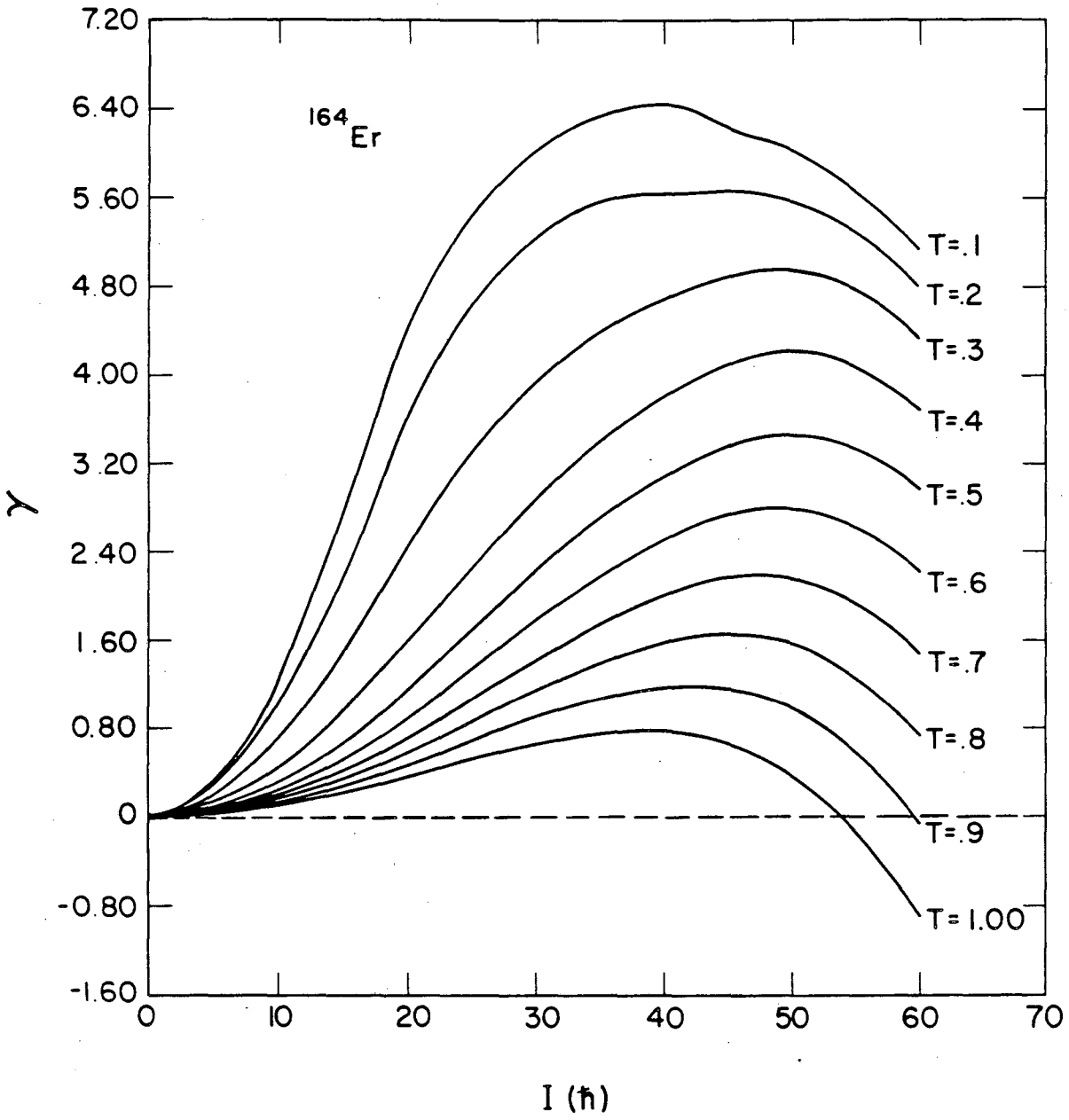

Fig. 6

XBL 8411-6391

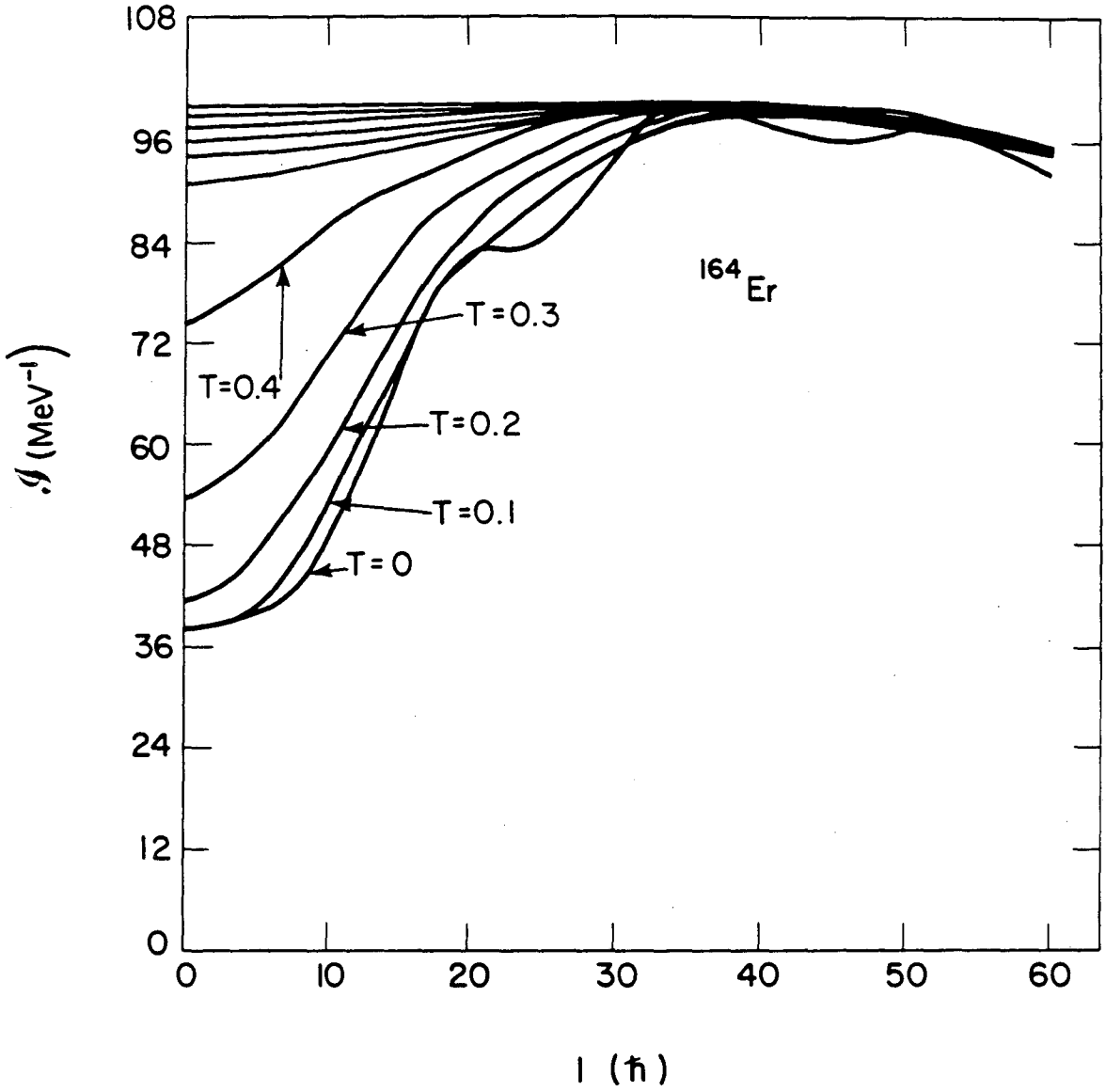

Fig. 7

XBL 8411-6388

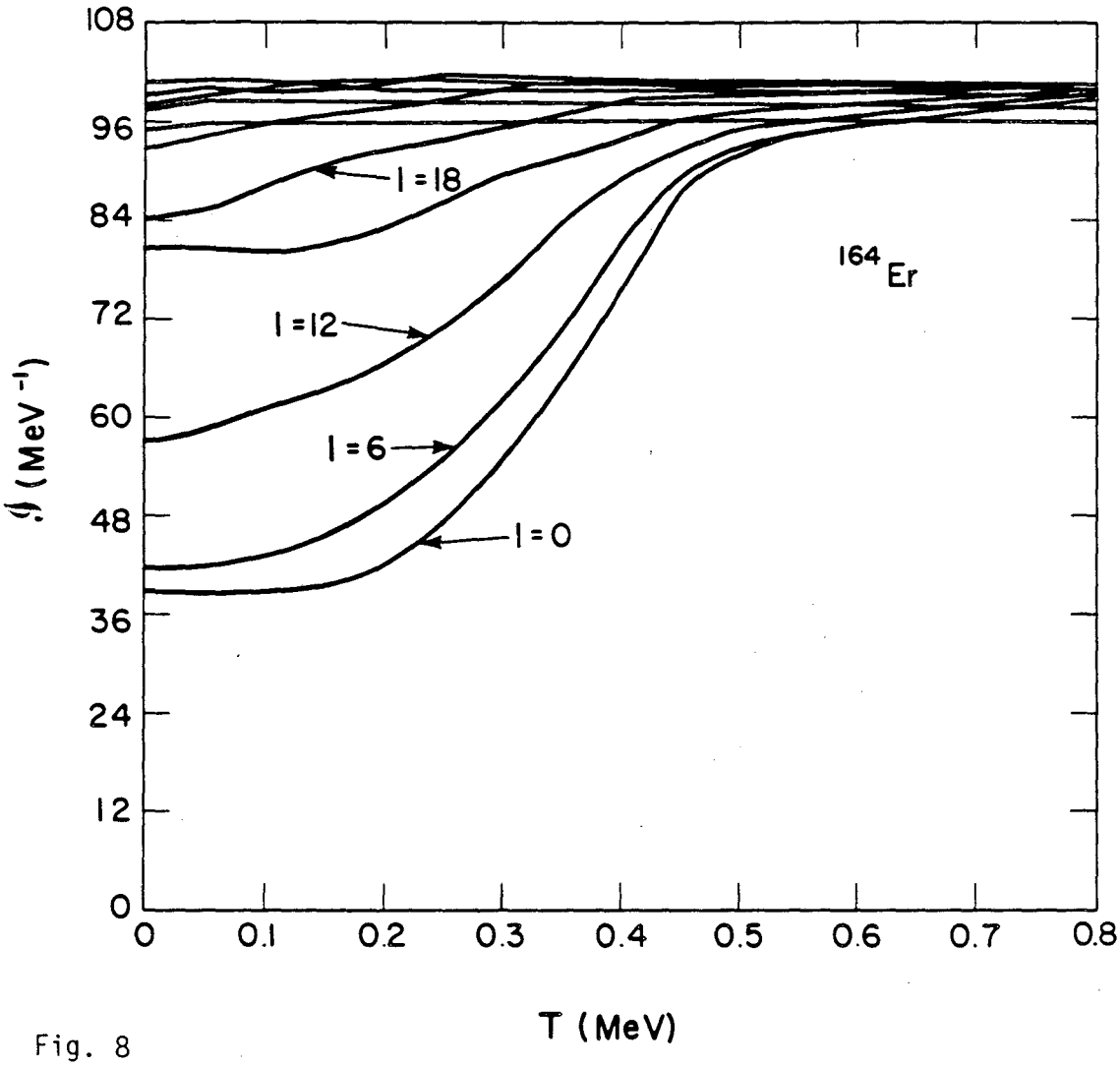

Fig. 8

XBL 8411-6392

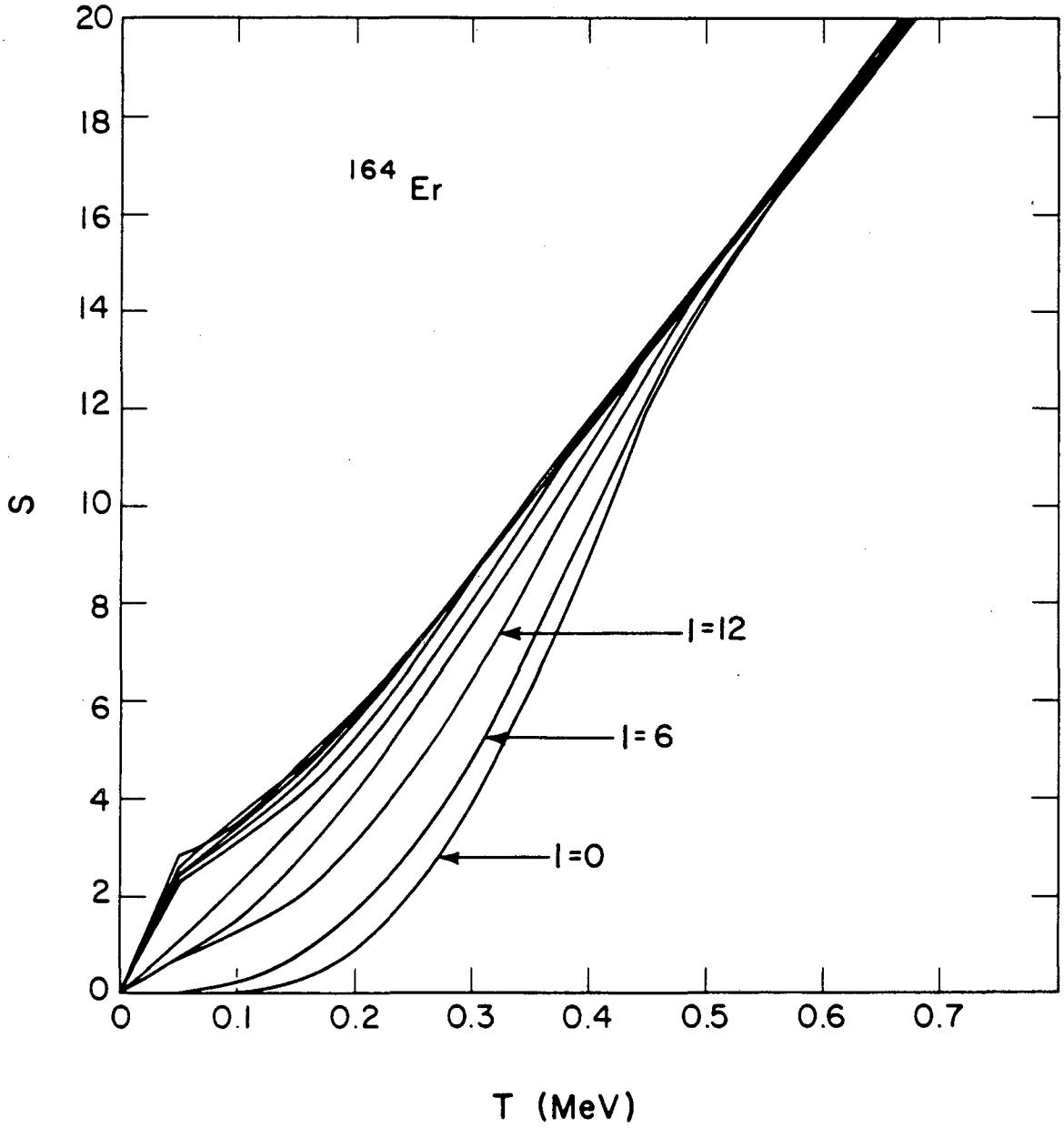

Fig. 9

XBL 8411-6393

This report was done with support from the Department of Energy. Any conclusions or opinions expressed in this report represent solely those of the author(s) and not necessarily those of The Regents of the University of California, the Lawrence Berkeley Laboratory or the Department of Energy.

Reference to a company or product name does not imply approval or recommendation of the product by the University of California or the U.S. Department of Energy to the exclusion of others that may be suitable.

LAWRENCE BERKELEY LABORATORY
TECHNICAL INFORMATION DEPARTMENT
UNIVERSITY OF CALIFORNIA
BERKELEY, CALIFORNIA 94720